



MINISTRY OF SUPPLY

AERONAUTICAL RESEARCH COUNCIL
REPORTS AND MEMORANDA

The Experimental Determination of the
Boundary Layer and Wake Characteristics
of a Piercy 12/40 Aerofoil, with Particular
Reference to the Trailing Edge Region

By

J. H. PRESTON, B.Sc., Ph.D., N. E. SWEETING and Miss D. K. Cox, B.Sc.
of the Aerodynamics Division, N.P.L.

Crown Copyright Reserved

LONDON : HIS MAJESTY'S STATIONERY OFFICE

Price 2s. 6d. net

The Experimental Determination of the Boundary Layer and Wake Characteristics of a Piercy 12/40 Aerofoil, with Particular Reference to the Trailing Edge Region

By

J. H. PRESTON, B.Sc., Ph.D., N. E. SWEETING and Miss D. K. COX, B.Sc.
of the Aerodynamics Division, N.P.L.

Reports and Memoranda No. 2013
26th February, 1945

1. *Summary.*—(a) *Reasons for Enquiry.*—To carry out on a Piercy 12/40 aerofoil an experimental investigation similar to that which was made using a Simple Joukowski aerofoil, and which is described in R. & M. 1998¹. The aim being to provide data relating to boundary layer and wake characteristics on two aerofoils, one cusped and the other with a finite trailing edge angle (22.1 deg.), from which a start could be made on the theoretical prediction of the chordwise load distribution taking due account of the boundary layer and wake, and to replace or substantiate the empirical corrections which were introduced in R. & M. 1996³, which describes an attempt to predict the lift of an aerofoil.

(b) *Range of Investigation.*—The tests were carried out on a 20-in. chord aerofoil in the 4-ft. No. 2 tunnel under conditions of zero interference. The Reynolds number was 0.42×10^6 .

θ/c , δ^*/c , δ/c , $H = \delta^*/\theta$ and the pressure rise through the boundary layer were obtained over the rear of the aerofoil and in the wake at 0 deg. and 6 deg., and in addition the trailing edge values of these quantities for either surface were determined at 3 deg. and 9 deg. Also detailed explorations of the static pressure variation in the neighbourhood of the trailing edge were made.

(c) *Conclusions.*—The general behaviour of these quantities as functions of position relative to the trailing edge at 0 deg. and 6 deg. incidence resembles that already obtained for the Simple Joukowski aerofoil of R. & M. 1998¹, the important feature being the comparatively rapid reduction in H and δ^* behind the trailing edge. The trailing edge values of these quantities as functions of incidence also show a somewhat similar behaviour to that obtained for the Joukowski aerofoil. It may be noted that H has attained a value of 2.4 without turbulent separation occurring. In the case of the Piercy aerofoil the pressure rise through the boundary layer at the trailing edge is much larger than is the case for the Joukowski aerofoil. Detailed traverses at the trailing edge are capable of yielding satisfactory drag measurements, with the additional advantage that the separate contributions of each surface can be obtained.

It is believed that these two reports give a fairly reliable picture of the variation of boundary layer and wake characteristics in the region of the trailing edge, in spite of the small Reynolds number 0.42×10^6 at which they were obtained. They will in any case be useful as guide for any future explorations which may be made at high Reynolds numbers.

2. *Introduction.*—This research is a parallel investigation to that described in R. & M. 1998¹, where boundary layer explorations were carried out on a symmetrical 12 per cent. Simple Joukowski aerofoil, which had a cusped trailing edge and its maximum thickness at 25 per cent. from the leading edge. The Piercy 12/40 aerofoil is also symmetrical. It has a maximum thickness of 12 per cent. occurring at 40 per cent. of the chord from the leading edge, and its trailing edge angle is 22.1 deg. It has therefore some of the features of a semi-low drag aerofoil, and its trailing edge shape approximates to those employed on closely balanced plain controls. The aerofoil was used in a previous investigation, described in R. & M. 2007², where the two-dimensional tunnel interference was determined by means of flexible walls which were adjusted to remove the interference.

Detailed reasons for these boundary layer explorations are given in the introduction to R. & M. 1998¹. Briefly, their purpose is to provide information on the magnitude and the mode of variation of the various boundary layer characteristics in the neighbourhood of the trailing edge, with a view to using them in calculations of lift and chordwise load distribution, where account is to be taken of the boundary layer, with the hope of obtaining a more intimate understanding of the effects of aerofoil shape, transition position and Reynolds number on the various sectional and control characteristics.

3. *Symbols and Definitions.*—These are listed in section 5 of R. & M. 1998¹.

4. *Range of Investigation.*—(a) *Previous Results for this Aerofoil.* The tests were carried out on a 26-in. chord aerofoil, at a wind speed of 40 ft. per second in the 4-ft. No. 2 tunnel, under conditions of zero interference. These were obtained by setting the flexible walls to the computed streamlines for the flow past the section, as is described in R. & M. 2007². The lift curves obtained with and without turbulence wires are shown in that report, as also are the pressure distributions for 0 deg., 3 deg., 6 deg. and 9 deg. incidence. The flow at the surface was observed by means of oil smoke. At speeds from 20 ft. per second to 60 ft. per second a marked laminar separation was observed on the lower surface from 0 deg. to 9 deg. incidence, whereas on the upper surface a normal transition from laminar to turbulent flow was observed. Curves are given in R. & M. 2007² showing the position of the transition and laminar separation and also the extent of the latter at 40 ft. per second. A peculiar hump in the lift curve above 6 deg. incidence was attributed to the laminar separation, because with the addition of turbulence wires near the nose a normal lift curve was obtained (see Fig. 3 of R. & M. 2007²).

(b) *Present Tests.*—Explorations of the boundary layer and wake at a number of stations in the neighbourhood of the trailing edge have been carried out at 0 deg. and 6 deg. incidence, whilst at 3 deg. and 9 deg. the exploration was limited to the trailing edge. The actual measurements were those of total head and static pressure in the boundary layer made by means of fine total head and static tubes traversed normal to the surface. At the trailing edge no normal exists, but the traverses were made approximately normal to the local streamlines. This was done by traversing along the bisector of the angle made by the surface of the aerofoil at the trailing edge and the chord-line produced. Corrections were made to the total head readings for the effective displacement of the centre of the pitot-tube mouth in a gradient of total head. From these traverses were obtained the velocity profiles, the boundary layer thickness (δ), the displacement thickness (δ^*), the momentum thickness θ , the ratio $H = \delta^*/\theta$, the pressure rise through the boundary layer and the velocity (or pressure) at the edge of the boundary layer. The absolute values of the static pressure readings may be in error, as it has been found that static pressures at the surface of the aerofoil obtained by extrapolating the static tube readings to this position differ (in the case of this aerofoil) from those recorded at a hole in the surface by about 3 per cent. of $\frac{1}{2}\rho U_0^2$. This appears to be an interference effect arising from the use of a static tube of finite dimensions near a surface of considerable curvature, and it is being made the subject of a separate note. It has no appreciable effect on the values of θ , δ^* , and H , but the pressure rise through the boundary layer near the trailing edge, and the static pressures near the edge of the boundary layer at this position should be treated with reserve.

5. *Results.*—(a) *Pressure Explorations.*—Figs. 1a, 2a, 3a and 4a show the measured pressure distribution along the chord line produced ahead of the aerofoil compared with theory corresponding to incidences of 0 deg., 3 deg., 6 deg. and 9 deg. These observations were used for the speed calibration by making use of the theoretical distribution, so that the excellent agreement obtained does to some extent depend on this.

Figs. 1b, 2b, 3b and 4b show the pressure distribution along normals to the chord line in the wake, except at the trailing edge where the traverses were made approximately normal to the streamlines. In the neighbourhood of the trailing edge a very considerable rise of pressure takes place through the boundary layer, and in this region the effect of adding turbulence wires to the nose of the wing is also marked. As has already been pointed out, the absolute magnitude of the recorded pressures close to the trailing edge may be in error owing to interference and curvature effects on the reading of a static tube close to a curved surface.

Figs. 1c and 3c show the pressure distribution in the centre of the wake at 0 deg. and 6 deg. incidence. These are everywhere less than theory even at distances of the order of $c/2$ from the trailing edge where the difference is of the order of $0.02-0.03$ of $\frac{1}{2}\rho U_0^2$. The measurements at 6 deg. incidence become negative at $0.4c$ from the trailing edge. At considerable distances from the trailing edge we should expect the pressures to tend to zero. Similar results were obtained in the case of the Joukowski aerofoil experiments¹. Theoretical calculations taking account of the boundary layer and wake show that a short distance behind the trailing edge ($0.1c$) the effect of the boundary layer and wake should be negligible so that the theoretical pressures should be obtained. This discrepancy requires some explanation. Mr. Fage suggested that a possible cause was the interference of the aerofoil boundary layer and wake on the tunnel wall boundary layers, causing the latter to thicken downstream and so produce an effective blockage. To test this a 2-ft. chord duralumin flat plate, $\frac{1}{8}$ -in. thick, was mounted in the 4-ft. tunnel at zero lift and static pressure explorations were carried out in the wake. At about $0.5c$ behind the trailing edge a pressure of $-0.02 \cdot \frac{1}{2}\rho U_0^2$ was recorded below that obtaining in the empty tunnel. The ends of the plate were then cut off so that there was no danger of the plate boundary layer mixing with the tunnel wall boundary layers for a distance of at least a chord behind the trailing edge. The plate was mounted on wires and the static pressures were again measured. The difference recorded at $0.5c$ behind the trailing edge was found to be $0.005 \cdot \frac{1}{2}\rho U_0^2$. This confirms Mr. Fage's idea, and it is evident that satisfactory comparisons with theory of pressures near the trailing edge and in the wake are going to be very difficult to obtain.

(b) *Velocity Profiles.*—Fig. 5a shows the velocity profiles at the trailing edge for the smooth aerofoil and for the aerofoil with turbulence wires near the nose, at incidences of 0 deg., 3 deg., 6 deg. and 9 deg. Wires have the greatest effect on the profiles for the lower surface and at 0 deg. and 3 deg. on the upper surface. At 6 deg. and 9 deg. the transition point is near the nose on the upper surface. It is evident that the upper surface velocity profiles for 9 deg. are near to turbulent separation forms, whilst the lower surface smooth wing profile at 9 deg. is near to a laminar separation profile.

(c) *Boundary Layer and Wake Characteristics at 0 deg. Incidence.*—Fig. 6a shows the displacement thickness δ^*/c . From $0.05c$ in front of the trailing edge to the trailing edge there is a rapid rise in δ^*/c , followed by a rapid reduction in the wake. Fig. 6b shows the momentum thickness θ/c which increases rapidly as the trailing edge is approached. Fig. 6c shows $H = \delta^*/\theta$. It will be noted that at $0.15c$ in front of the trailing edge H reaches a value of 4.7 for the smooth aerofoil; this is in accordance with the presence of laminar separation on this surface. The flow then becomes turbulent and rejoins the surface before the trailing edge is reached. With turbulence wires in position, H is constant = 1.55, over the rear of the wing to within $0.05c$ of the trailing edge when it commences to rise because of the adverse pressure gradient. Fig. 6d shows the boundary layer thickness δ/c which also shows a rapid rise as the trailing edge is approached. Finally, Fig. 6e shows the pressure rise through the boundary layer. In the neighbourhood of the trailing edge this is positive and large—much larger than was observed for the Simple Joukowski aerofoil. This can be attributed to the comparatively large trailing edge angle of this section.

(d) *Boundary Layer and Wake Characteristics at 6 deg. Incidence.*—These have been determined for the "wires on" case only, as the presence of laminar separation on the lower surface is an added complication which it is desirable to avoid for the present. On the other hand a strict comparison with the results obtained for the Joukowski aerofoil cannot be obtained, as in the latter case the exploration at 6 deg. incidence was carried out for the smooth wing only.

The wake results have been analysed for the upper and lower parts of the wake with a dividing line coincident with the position of the minimum total head. This gives some idea as to how the upper and lower boundary layers on the wing merge together to form the wake.

The results are shown on Figs. 7a-7c. As one would expect the values of the displacement thickness δ^* , momentum thickness θ and boundary thickness are greater for the upper surface than the lower surface, and for both surfaces the values rise rapidly as the trailing edge is approached. The ratio $\delta^*/\theta = H$ is also greater for the upper surface, and for both surfaces it rises as the trailing edge is approached. Behind the trailing edge δ^* , θ and H for the upper surface decrease rapidly at first and then more gradually, tending to a constant value at considerable distances from the trailing edge. The values for the lower portion continue to rise for a short distance behind the trailing edge where a maximum is reached. They then fall, gradually approaching the "upper surface" values. In the case of H , the values are identical for the two halves of the wake at, and beyond, $0.025c$ from the trailing edge. In the case of the boundary layer thickness δ (Fig. 7d) there is a rapid fall of the upper part just behind the trailing edge, it then gradually reaches a minimum and commences to rise again slowly. The lower boundary layer thickness rises rapidly as the trailing edge is approached and behind the trailing edge continues to rise slowly and approach the upper part. As for the pressure rise through the boundary layer (Fig. 7e), the maximum value is reached at the trailing edge and is roughly the same for both surfaces. Ahead of the trailing edge there is a slight fall of pressure through the boundary layer, the change from positive to negative is comparatively rapid for the lower surface and occurs nearer to the trailing edge than is the case for the upper surface.

(e) *Comparison of Results in the Wake at 0 deg. and 6 deg. Incidence.*—Figs. 8a-8c show the variation of θ/c , δ^*/c and H against distance behind the trailing edge. The general behaviour is similar for both incidences. Fig. 8c shows the drag as computed at various sections of the wake by B. M. Jones's formula. This has come out remarkably constant in all four cases and shows that even traverses at the trailing edge can yield a reliable value for the drag if sufficient total head observations are taken. Fig. 8f shows the variation of velocity at the wake centre with distance behind the trailing edge, and Fig. 8g shows the variation of wake width with distance behind the trailing edge. The general behaviour of all the quantities listed here is in accord with that of previous experiments on a Simple Joukowski aerofoil.

(f) *Results from the Trailing Edge Traverses for each Surface as Functions of Incidence.*—Figs. 9a-9f show the variation with incidence of C_D , δ^*/c , θ/c , $H = \delta^*/\theta$, δ/c , $(U_1/U_0)^2$ and $\Delta p/\frac{1}{2}\rho U_0^2$ for each surface at the trailing edge with and without turbulence wires. It is assumed as in the case of the Simple Joukowski tests that $2\int_0^{\delta/c} (g - p)^{1/2} (1 - \sqrt{g}) d(n/c)$ taken across the boundary layer at the trailing edge gives the C_D for that surface.

The curves of C_D , δ^*/c , θ/c and δ/c are very similar to each other. The lower surface results show only a slow variation with incidence whilst for the upper surface they increase rapidly. In this respect they differ from the Simple Joukowski tests of R. & M. 1998¹. The upper surface values at 6 deg. and 9 deg. with and without wires do not differ much and this is to be expected as at these incidences the transition point has moved forward to the nose (see Fig. 2 of R. & M. 2007²). The results at 9 deg. on the lower surface with wires tend to approach the smooth aerofoil results. This is thought to be due to the effect of the extensive favourable pressure gradient on the lower surface damping out the disturbances caused by the wire and producing an intermediate regime of laminar flow.

$H (= \delta^*/\theta)$ ranges from 1.6 on the lower surface at 9 deg. to 2.4 on the upper surface at 9 deg. for the case of turbulence wires at the nose. It may be noted that separation has not occurred at this incidence. For the smooth aerofoil, the values of H for the upper surface tend to approach those obtained with turbulence wires; but on the lower surface a value of $H = 3.8$ is reached at 9 deg. indicating conditions near to laminar separation, which agrees with the smoke observations.

Fig. 9f shows the pressure rise through the boundary layer at the trailing edge for either surface as a function of incidence. This is a maximum at 0 deg. incidence. Addition of turbulence wires gives rise to a much smaller variation with incidence. On the same figure is shown the velocity at the edge of the boundary layer at the trailing edge—actually $(U_1/U_0)^2$. This rises

in a parabolic manner with increase of incidence. It is of considerable interest in calculations of lift, in which account is taken of the effect of the boundary layer (*see* R. & M. 1996³), since $(U_1/U_0)^2$ is closely related to the rate at which vorticity from a particular surface is being discharged into the wake.

(g) *Boundary Layer Thickness at the Trailing Edge as a Function of the Drag.*—This is shown in Fig. 10, which was obtained by eliminating the incidence from Figs. 9a and 9e. The corresponding curve obtained for the Simple Joukowski aerofoil of R. & M. 1998¹ is also shown. Some points communicated by Mr. Squire of the Royal Aircraft Establishment, obtained from flight tests for a C_L range of 0.2 to 0.4 and a Reynolds number range of 6.0×10^6 to 8.0×10^6 have been included. The results were obtained from traverses made at $0.01c$ behind the trailing edge. The three curves lie close together and it would seem that, within the present limits of experimental accuracy, the boundary layer thickness at the trailing edge is a universal function of the corresponding drag, being independent of aerofoil shape, incidence, boundary layer conditions and presumably Reynolds number. This is of considerable importance, since fairly reliable estimates of the effect of transition position and Reynolds number on drag can be obtained, and hence by means of Fig. 10 the effect of these on the boundary layer thickness at the trailing edge can be estimated.

(h) *Results from the Trailing Edge Traverses for the Wake as a Whole, as Functions of Incidence.*—Figs. 11a-11e show the variation with incidence of δ^*/c , θ/c , $H = \delta^*/\theta$, δ/c and C_D for the wake at the trailing edge. The variation is roughly parabolic for the incidence range shown here. The effect of adding turbulence wires at the nose is appreciable, especially at small incidences. Fig. 11f shows the variation of the pressure at the trailing edge with incidence. This pressure falls as the incidence increases, in a parabolic manner. The absolute values of the pressure coefficient are uncertain because of the rapidly changing curvature of the streamlines in the neighbourhood of the trailing edge which affects the reading of the static tube.

Fig. 11g shows the variation of $(U_U/U_L)^2$ with incidence, where U_U denotes the velocity at the edge of the boundary layer on the upper surface, and U_L that for the lower surface. With turbulence wires the ratio is very closely equal to unity, and for the smooth aerofoil falls to 0.98 at 6 deg. incidence and then rises to 1.015 at 9 deg. incidence. It was shown in R. & M. 1996³, that, for a lifting aerofoil, equal amounts of positive and negative vorticity must be discharged into the wake at the trailing edge. The rate at which vorticity is discharged into the wake from say the upper surface was shown to be given approximately by $-\frac{1}{2}U_U^2$ and from the lower surface by $+\frac{1}{2}U_L^2$. Hence to this degree of approximation equal discharge of positive and negative vorticity leads to the equation

$$(U_U/U_L)^2 = 1.0,$$

which is closely confirmed by experiment.

6. *Conclusions.*—Dealing first with the pressure distributions. Ahead of the model along the chord line produced, the pressures (or velocities) are in excellent agreement with theory. In the wake, discrepancies are observed which tend to increase with distance from the trailing edge. Theory, which allows for the boundary layer and wake, shows that beyond $0.1c$ behind the trailing edge departures from potential flow theory should be negligible. The discrepancy has been traced to the interference between the wing boundary layer and the tunnel wall boundary layers. This results in an increased blockage, thus lowering the static pressure. Traverses through the boundary layer at the trailing edge show that the pressure rise through the boundary layer for this aerofoil is much greater than for the Simple Joukowski aerofoil (*see* R. & M. 1998¹). This can be attributed to the finite trailing edge angle of the Piercy 12/40 aerofoil. Pressures in this region are below those of potential flow, but show similar trends. There is an unknown error in the recorded pressures near the trailing edge, because of curvature effects in the reading of a static tube near a surface.

The variation of the shape of the velocity profile in the wake shows the same features as were observed in the case of the Simple Joukowski aerofoil¹; namely, near the trailing edge the changes of shape are confined to the centre of the wake, followed by a gradual broadening of the wake with gentler velocity variations across it. We may note that even at 9 deg. incidence the trailing edge velocity profiles show no signs of separation.

The boundary layer and wake characteristics are also very similar to those observed on the Joukowski aerofoil.¹ In particular, the rapid decrease of δ^* and $H (= \delta^*/\theta)$ immediately after the trailing edge may again be noted. In the case of the Piercy 12/40 aerofoil θ , δ^* , H , and δ all rise rapidly as the trailing edge is approached. This is due to the steep unfavourable pressure gradient. It may be noted that well ahead of the trailing edge, where the pressure gradients are small, H is almost constant and has a value of about 1.55, which agrees well with that obtained for the Simple Joukowski aerofoil. In theoretical work H has frequently been assumed to have a value of 1.4, where the pressures are small. In point of fact H is a function of Reynolds number. The present tests were made at $R = 0.42 \times 10^6$ and $H = 1.4$ roughly corresponds to $R = 10^6$. A feature which is worth calling attention to is the presence of a fairly strong laminar separation on the lower surface at all positive incidences (see Fig. 2 of R. & M. 2007²). The other important point is that as in the case of the Simple Joukowski aerofoil, the drag can be obtained with ample accuracy from trailing edge traverses, provided the total head variation is explored in sufficient detail. There may be difficulties in doing this in flight with a comb. On the other hand a trailing edge traverse does enable the drag contribution of the upper and lower surfaces to be found separately.

From traverses at the trailing edge, the variations of C_D , θ , δ^* , H , etc., with incidence show very similar features to those obtained in the case of the Joukowski aerofoil. We may note that at 9 deg. on the upper surface H has attained a value of 2.4 without turbulent separation occurring. Also at 9 deg. on the lower surface it appears that the turbulence wire at the nose is not large enough to ensure completely turbulent flow over this surface. When the trailing edge boundary layer thickness for a particular surface is plotted against the corresponding C_D , a curve is obtained which is independent of transition position and incidence. This curve is only slightly above the similar curve obtained for a Simple Joukowski aerofoil. Mr. Squire of the R.A.E. has obtained a similar result from the analysis of traverses made 0.01c behind a 15 per cent. EQ wing in flight, where R ranged from 6.0×10^6 to 8.0×10^6 . These points lie slightly below the curve for the Simple Joukowski aerofoil in a C_D range of 0.002 to 0.006. We can therefore assume, in view of the difficulties of estimating δ , that a universal relation exists between δ and the corresponding C_D , which is approximately independent of aerofoil shape, incidence, boundary layer conditions, and Reynolds number. This is important, as it enables a reliable estimate of δ at the trailing edge to be made, when C_D is known. Finally, it has been found, as in the case of the Simple Joukowski aerofoil, that the velocities at the edge of the boundary layer on opposite sides of the trailing edge are closely equal, thus approximately verifying the theorem that equal amounts of positive and negative vorticity must be discharged into the wake.

7. *Further Developments.*—The work described in this report and in R. & M. 1998¹ should provide enough data to enable calculations of pressure at the edge of the boundary layer, and of the pressure rise through the boundary layer to be made, and ultimately to extend the lift calculations of R. & M. 1996³ with a view to obtaining the chordwise load distribution and hence the hinge moments and pitching moments. These calculations should throw considerable light on the action of the boundary layer in conjunction with convex and concave control surfaces on lift and hinge moments.

A start has already been made on the flow past a symmetrical aerofoil at 0 deg. incidence, taking account of the boundary layer and wake. It has been found that, except near the trailing edge, these have negligible effects, so that the pressures or velocities *outside* the boundary layer and wake are almost identical with those computed by elementary potential flow theory. The computed pressure rise through the boundary layer at the trailing edge is in qualitative agreement with experiment, being in fact somewhat greater, but the discrepancies might well be accounted for by the difficulties of measuring the true static pressure in this region.

REFERENCES

- | <i>No.</i> | <i>Author</i> | <i>Title</i> |
|------------|---|--|
| 1 | Preston, J. H. and Sweeting, N. E. . . | The Experimental Determination of the Boundary Layer and Wake Characteristics of a Simple Joukowski Aerofoil with Particular Reference to the Trailing Edge Region. R. & M. 1998. (March, 1943.) |
| 2 | Preston, J. H., Sweeting, N. E. and Miss D. K. Cox. | The Experimental Determination of the Two-dimensional Interference on a Large Chord Piercy 12/40 Aerofoil in a Closed Tunnel fitted with Flexible Roof and Floor. R. & M. 2007. (Sept., 1944.) |
| 3 | Preston, J. H. | The Approximate Calculation of the Lift of Symmetrical Aerofoils taking Account of the Boundary Layer, with Application to Control Problems. R. & M. 1996. (May, 1943.) |
-

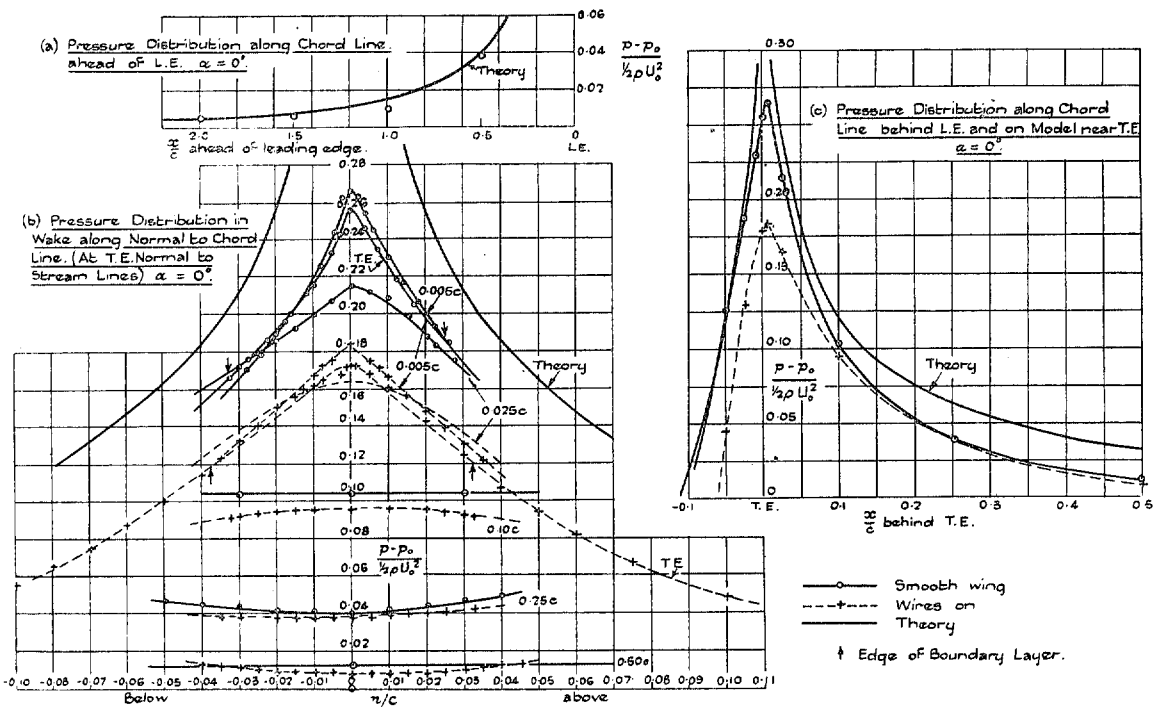


FIG. 1.—Pressure Distributions at $\alpha = 0$ deg.

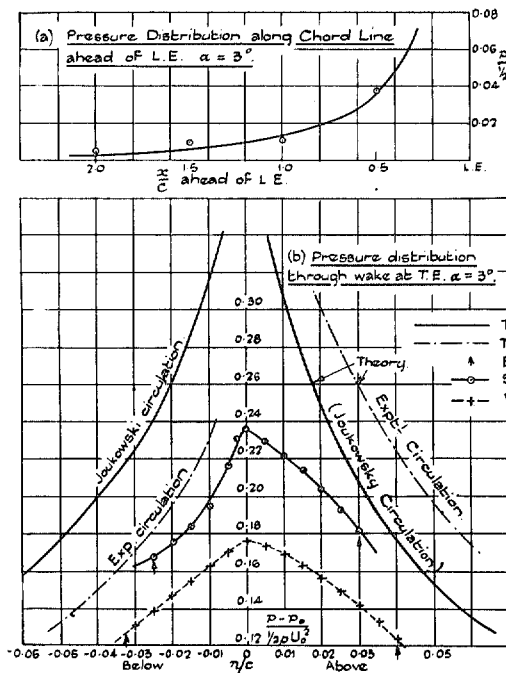


FIG. 2.—Pressure Distributions at $\alpha = 3$ deg.

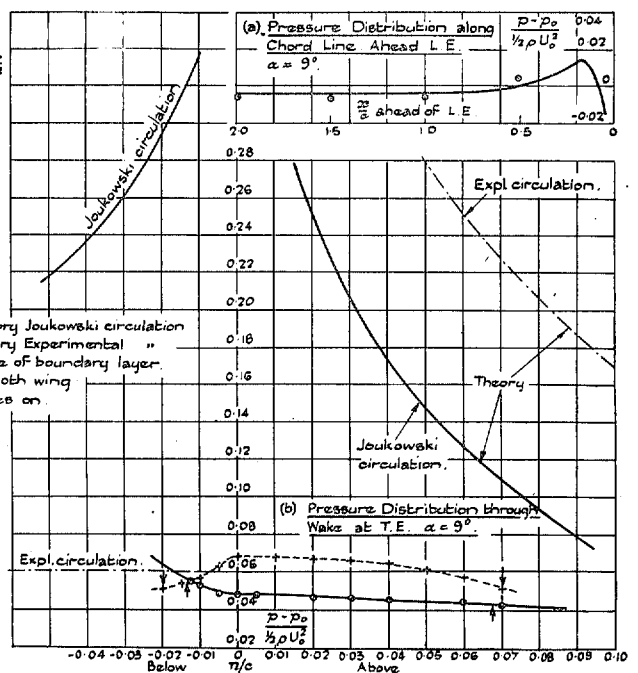


FIG. 4.—Pressure Distributions at $\alpha = 9$ deg.

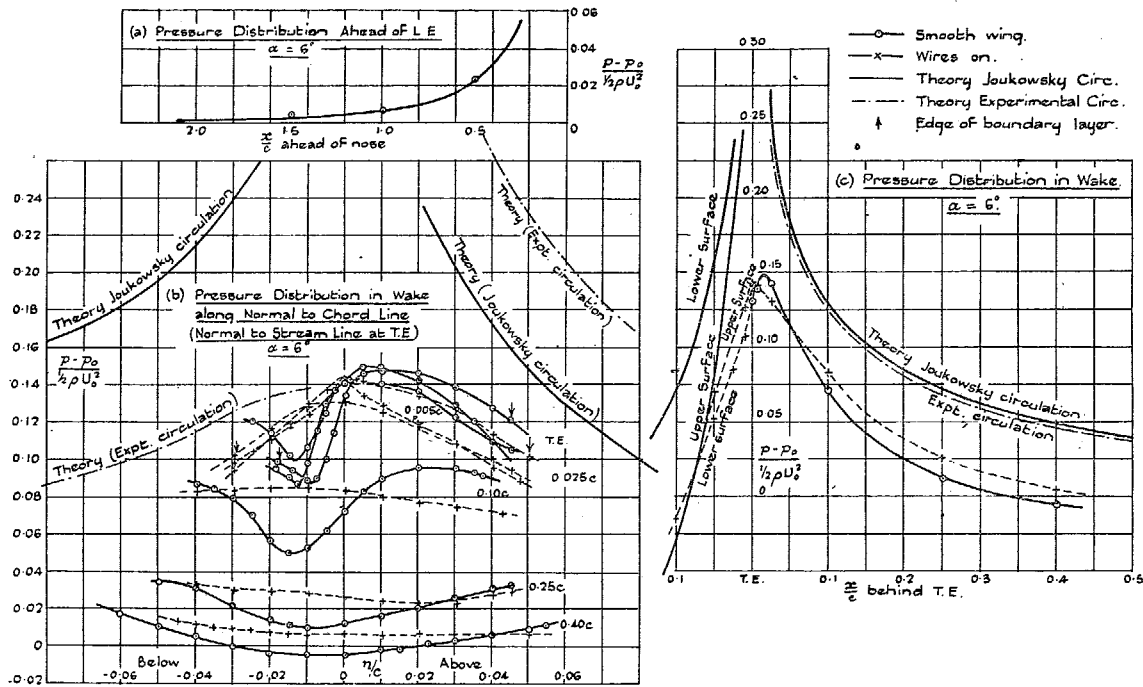


FIG. 3.—Pressure Distributions at $\alpha = 6$ deg.

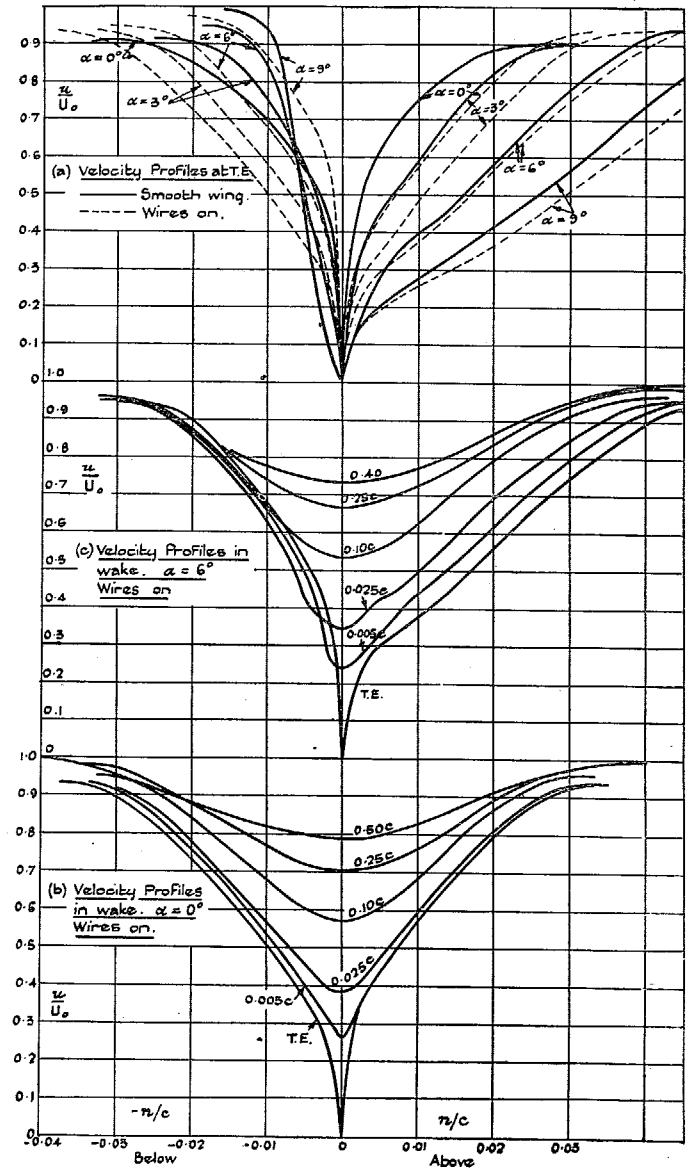


FIG. 5.—Velocity Profiles.

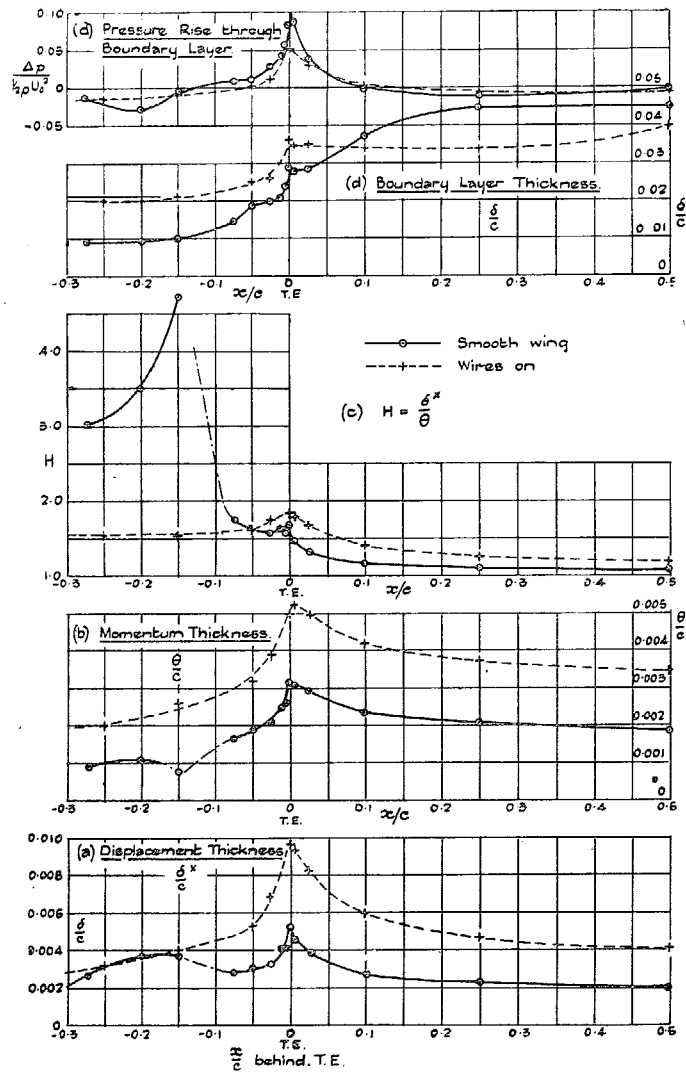


FIG. 6.—Variation in δ^*/c , θ/c , H , δ/c and Pressure Rise Through Boundary Layer. $\alpha = 0$ deg., One Surface.

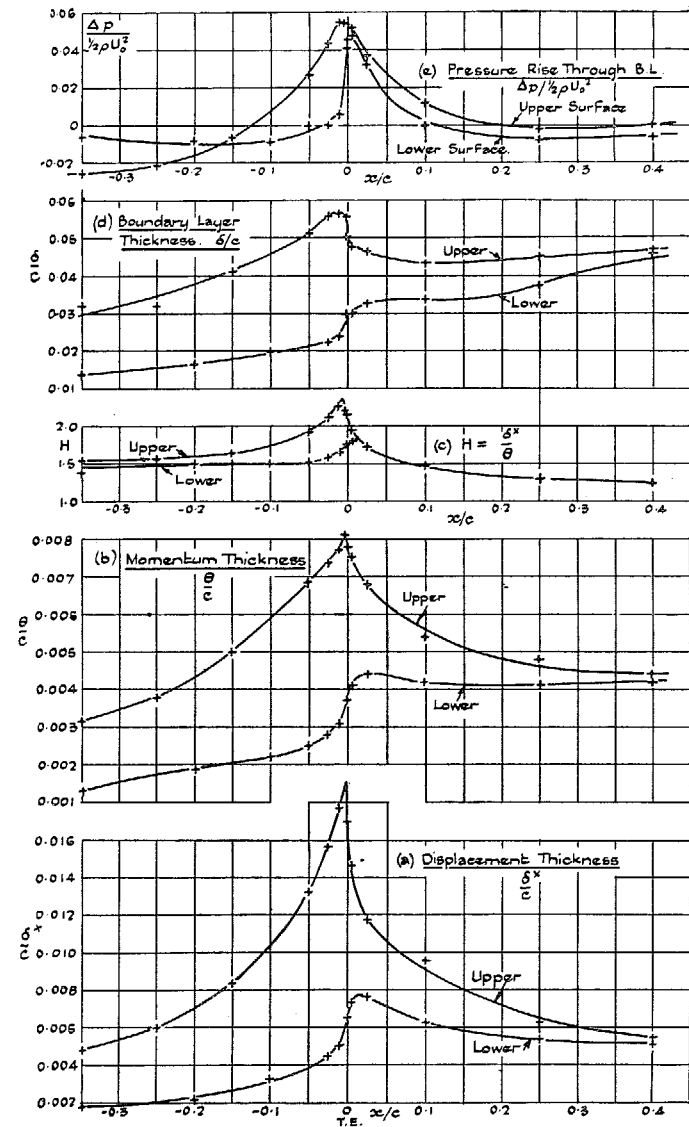


FIG. 7.— $\alpha = 6$ deg. wires on. Variations in δ^*/c , θ/c , H , δ/c and $\Delta p / \frac{1}{2} \rho U_0^2$ over the Aerofoil and in the Wake.

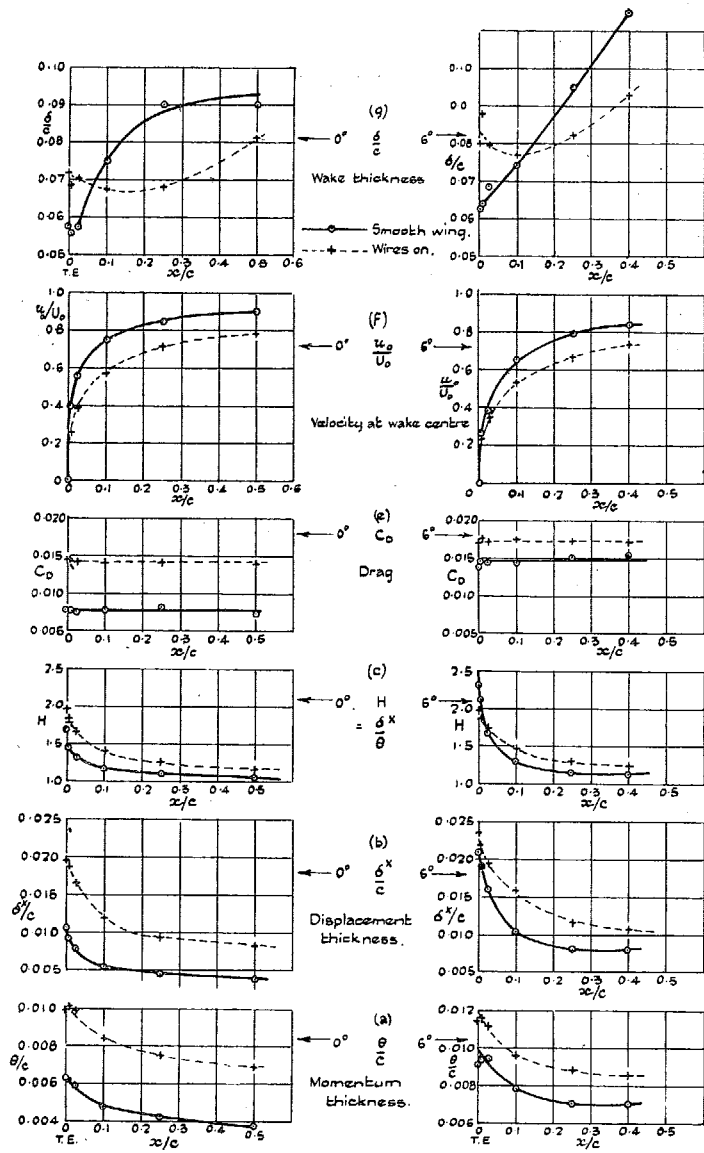
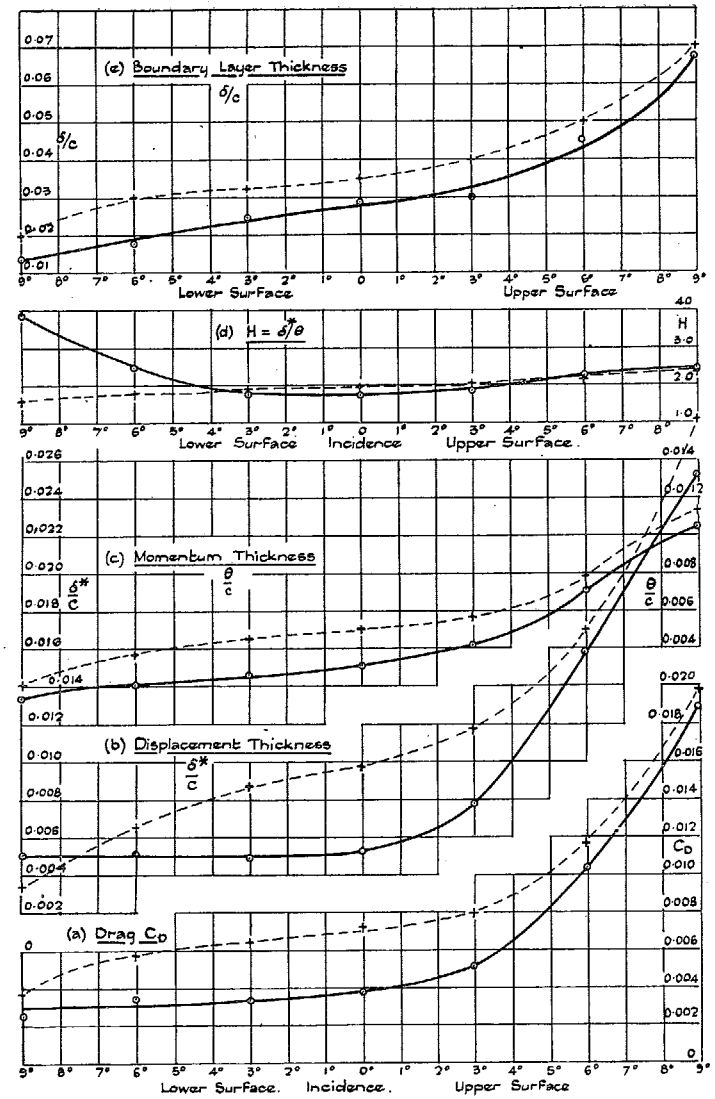


FIG. 8.—Variation of δ^*/c , θ/c , H , C_D , u_w/U_0 and δ/c in the Wake at 0 deg. and 6 deg. incidence.



FIGS. 9a—9d.

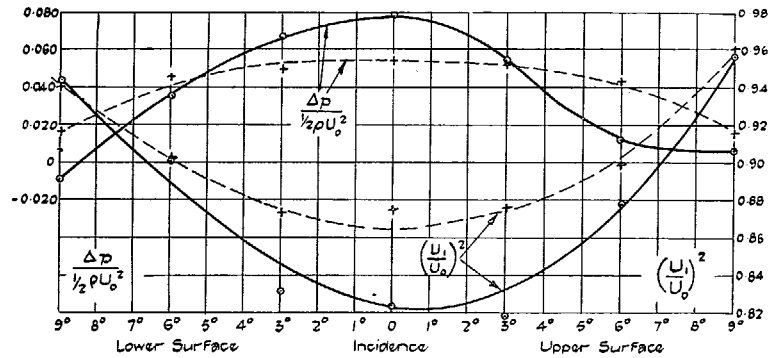


FIG. 9f.

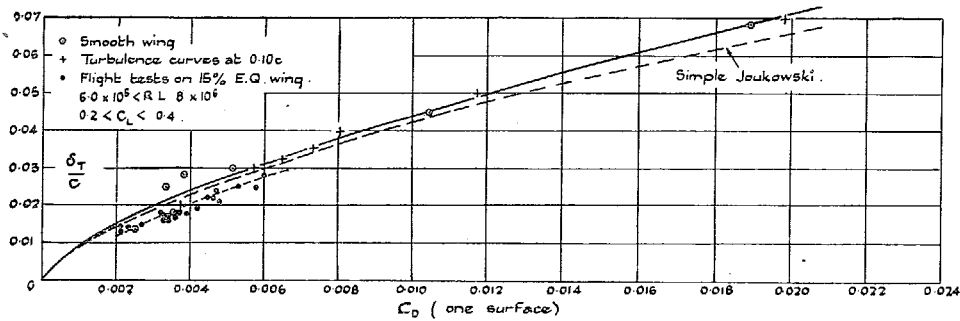


FIG. 10.

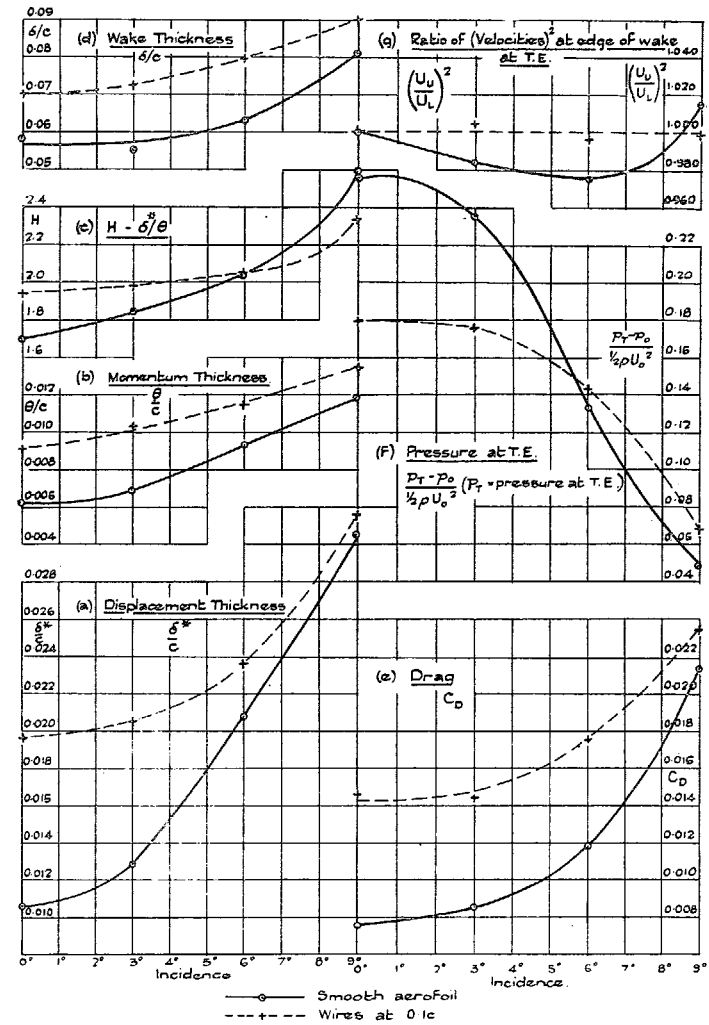


FIG. 11.—Variations of δ/c^* , θ/c , H , δ/C , C_D , Pressures at T.E., and Ratio of (Velocities)² at Edge of Wake.

Publications of the Aeronautical Research Committee

TECHNICAL REPORTS OF THE AERONAUTICAL RESEARCH COMMITTEE—

- 1934-35 Vol. I. Aerodynamics. 40s. (40s. 8d.)
Vol. II. Seaplanes, Structures, Engines, Materials, etc.
40s. (40s. 8d.)
- 1935-36 Vol. I. Aerodynamics. 30s. (30s. 7d.)
Vol. II. Structures, Flutter, Engines, Seaplanes, etc.
30s. (30s. 7d.)
- 1936 Vol. I. Aerodynamics General, Performance,
Airscrews, Flutter and Spinning.
40s. (40s. 9d.)
Vol. II. Stability and Control, Structures, Seaplanes,
Engines, etc. 50s. (50s. 10d.)
- 1937 Vol. I. Aerodynamics General, Performance,
Airscrews, Flutter and Spinning.
40s. (40s. 9d.)
Vol. II. Stability and Control, Structures, Seaplanes,
Engines, etc. 60s. (61s.)

ANNUAL REPORTS OF THE AERONAUTICAL RESEARCH COMMITTEE—

- 1933-34 1s. 6d. (1s. 8d.)
1934-35 1s. 6d. (1s. 8d.)
April 1, 1935 to December 31, 1936. 4s. (4s. 4d.)
1937 2s. (2s. 2d.)
1938 1s. 6d. (1s. 8d.)

INDEXES TO THE TECHNICAL REPORTS OF THE ADVISORY COMMITTEE ON AERONAUTICS—

December 1, 1936 — June 30, 1939
Reports & Memoranda No. 1850. 1s. 3d. (1s. 5d.)

July 1, 1939 — June 30, 1945
Reports & Memoranda No. 1950. 1s. (1s. 2d.)

Prices in brackets include postage.

Obtainable from

His Majesty's Stationery Office

London W.C.2 : York House, Kingsway
[Post Orders—P.O. Box No. 569, London, S.E.1.]

Edinburgh 2: 13A Castle Street

Manchester 2: 39-41 King Street

Cardiff: 1 St. Andrew's Crescent

Belfast: 80 Chichester Street

or through any bookseller.